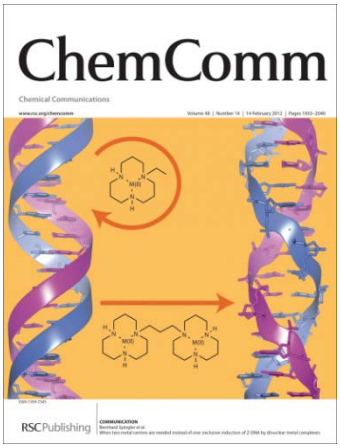

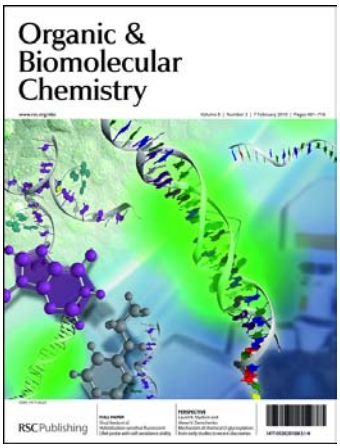

This article is part of the

Nucleic acids: new life, new materials

web-themed issue

Guest edited by:

Mike Gait Medical Research Council, Cambridge, UK	**Ned Seeman** New York University, USA	**David Liu** Harvard University, USA	**Oliver Seitz** Humboldt-Universität zu Berlin, Germany	**Makoto Komiyama** University of Tsukuba, Japan	**Jason Micklefield** University of Manchester, UK

All articles in this issue will be gathered online at

www.rsc.org/nucleic_acids

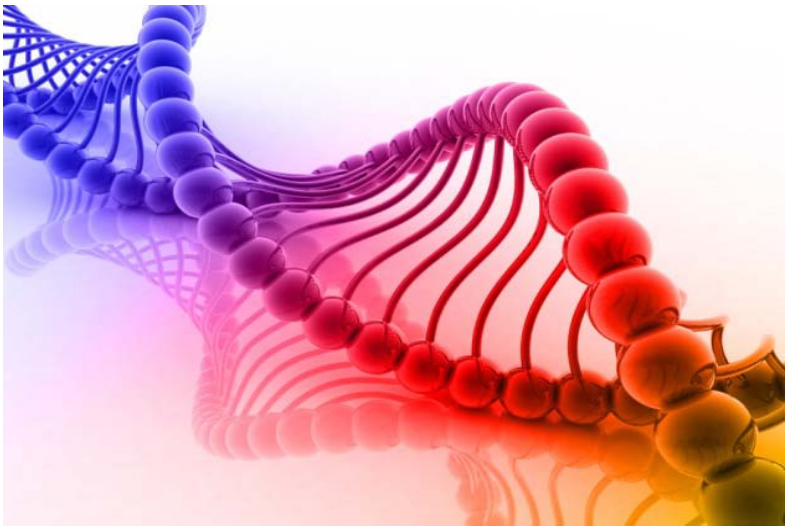

Organic & Biomolecular Chemistry

Dynamic Article Links

Cite this: *Org. Biomol. Chem.*, 2012, **10**, 7363

www.rsc.org/obc

PAPER

Dual fluorophore PNA FIT-probes – extremely responsive and bright hybridization probes for the sensitive detection of DNA and RNA†

Elke Socher, Andrea Knoll and Oliver Seitz*

Received 14th May 2012, Accepted 10th July 2012
DOI: 10.1039/c2ob25925g

Fluorescently labeled oligonucleotides are commonly employed as probes to detect specific DNA or RNA sequences in homogeneous solution. Useful probes should experience strong increases in fluorescent emission upon hybridization with the target. We developed dual labeled peptide nucleic acid probes, which signal the presence of complementary DNA or RNA by up to 450-fold enhancements of fluorescence intensity. This enabled the very sensitive detection of a DNA target (40 pM LOD), which was detectable at less than 0.1% of the beacon concentration. In contrast to existing DNA-based molecular beacons, this PNA-based method does not require a stem sequence to enforce dye–dye communication. Rather, the method relies on the energy transfer between a "smart" thiazole orange (TO) nucleotide, which requires formation of the probe–target complex in order to become fluorescent, and terminally appended acceptor dyes. To improve upon fluorescence responsiveness the energy pathways were dissected. Hydrophobic, spectrally mismatched dye combinations allowed significant (99.97%) decreases of background emission in the absence of a target. By contrast, spectral overlap between TO donor emission and acceptor excitation enabled extremely bright FRET signals. This and the large apparent Stokes shift (82 nm) suggests potential applications in the detection of specific RNA targets in biogenic matrices without the need of sample pre-processing prior to detection.

Introduction

A variety of fluorescence-labeled oligonucleotide probes allow the homogeneous detection of nucleic acid targets and thereby simplify assays when separation of unbound from bound probes is difficult.[1,2] Such measurements are required in various fields concerned with basic research, drug development, medical diagnosis, food security and others. The analysis of nucleic acid samples from biological fluids such as blood, cell lysates or whole cells is complicated by the high fluorescence background. High signal-to-background ratios are required, especially for targets of low abundance. Thus, useful probes should signal the presence of a specific nucleic acid target by strong enhancements of fluorescence upon binding. DNA molecular beacons present a remarkable solution to the problem.[3,4] These hairpin-shaped probes take advantage of the distance-dependent interaction between two chromophores (Fig. 1a). In the absence of a target, two dyes are forced into close proximity by means of self-complementary arm sequences. The fluorescence background is low because the emission is effectively quenched by fluorescence resonance energy transfer (FRET), collisional quenching, and/or formation of ground- or excited-state complexes. Hybridization with a complementary target opens the hairpin structure. The dyes are separated and fluorescence is restored. Molecular beacons have been used on arrays,[5] in the real-time detection of DNA formed in PCR[6,7] and NASBA[8] and for the detection of RNA in live cells.[9] However, the detection of minor amounts of specific DNA or RNA sequences remains a challenge.

In DNA molecular beacons, the dye molecules typically are attached to the terminal ends of the oligonucleotide probe. End-fraying can cause incomplete quenching of fluorescence, which may lead to increases of background fluorescence in the absence of a target. Various approaches for improvements of the signal-to-background ratios of fluorescent hybridization probes have been reported which include wavelength-shifting beacons,[10] FRET-based beacons,[11] super-quenched beacons,[12] nanoparticle quenched beacons,[13] triplex-stem beacons,[14] mercury enhanced beacons,[15] in-stem beacons[16–18] and excimer-controlled and excimer-signaling beacons.[19–22] In the hairpin-shaped molecular beacons the stem region is a critical design element. Large fluorescence enhancements upon hybridization can only be obtained with stem segments that are readily opened. However, unintended dissociation of the stem, for example by binding of mismatched targets or other biomolecules, has to be avoided. This requires stable stem regions. Thus, the criteria for the stem design are ambiguous.

Department of Chemistry, Humboldt University Berlin, Brook-Taylor-Str. 2, 12489 Berlin, Germany. E-mail: oliver.seitz@chemie.hu-berlin.de; Fax: +49 30 20937266; Tel: +49 30 20937446

†Electronic supplementary information (ESI) available: Synthesis and characterization data of PNA probes. See DOI: 10.1039/c2ob25925g

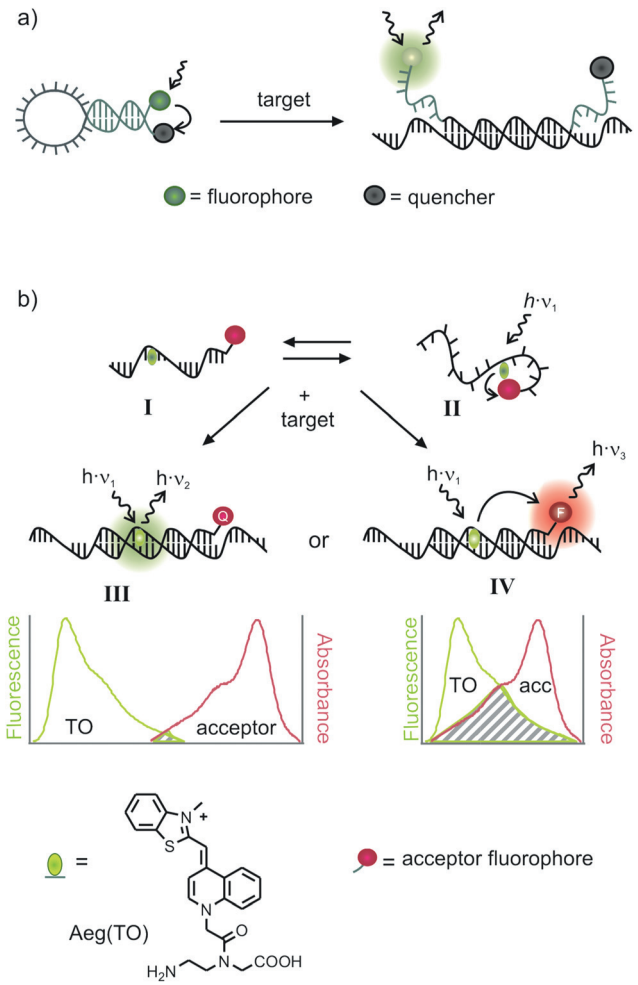

Fig. 1 Signaling of probe hybridization by (a) molecular beacons and (b) dual fluorophore PNA FIT-probes. The PNA FIT-probes are flexible in the single-stranded state (I and II). This enables donor–acceptor contacts, which quench fluorescence emission. Furthermore, the thiazole orange dye (TO) requires double strand formation in order to become highly fluorescent. Thus, fluorescence intensity in the single strand is low and increases after hybridization to a complementary target due to stacking of TO with the formed base pairs. Acceptor fluorophores Q which provide little spectral overlap improve the responsiveness of TO emission (III). An overlap between absorbance of acceptors F and TO emission spectra yields FRET (IV).

We, and others, have introduced fluorogenic PNA probes, which signal hybridization despite the absence of stem regions. In the so-called PNA FIT (forced intercalation)-probes, the cyanine dye thiazole orange (TO) serves as an artificial nucleobase and is forced to intercalate at a desired position of the probe–target duplex.[23–27] Intercalation restricts torsional motions around the central methine bridge and prevents rapid depletion of the TO excited state.[28] PNA FIT-probes enable single base specific calls because fluorescence enhancements are only obtained when TO is flanked by matched base pairs. This has facilitated applications in real-time PCR genotyping, RNA detection[29] and live cell RNA imaging.[30–33] The PNA FIT-probes achieved up to 30-fold enhancement of TO emission and enabled the detection of 0.5 nM DNA. Concomitant with PNA FIT-probes[27] the PNA Light-Up probes have been developed.[31,32] In PNA Light-Up probes, the TO hangs *via* the terminus of PNA by means of a flexible tether.[34,35] These probes provided up to 50-fold enhancements of TO emission upon formation of triplexes. Labeling at the periphery of DNA by TO dimers yielded probes that show quenched exciton emission in the single stranded state and monomer emission upon hybridization.[36] The so-called ECHO probes have a tendency to form self-dimers.[37] TO has also been introduced at internal positions of oligonucleotides.[38–42] We[43] and others[44,45] introduced stem-less PNA beacons which respond to global changes of conformation. The high flexibility of single stranded PNA facilitates collisions between two dyes. Hybridization of dual labeled PNA is accompanied by fluorescence enhancements because the rigid probe–target duplex prevents collisional quenching. However, the 10-fold increases of fluorescence upon hybridization are low when compared to TO-based PNA probes. To improve the signal-to-background ratio, we took advantage of our original FIT-probe concept and added a second fluorophore, the near-infrared (NIR) dye NIR664, which served as an acceptor dye (Fig. 1b).[46] This design provided extremely low fluorescence of the unbound state (background) because the low fluorescence of unstacked TO was further reduced by energy transfer with the NIR664-dye (acceptor). Hybridization was accompanied by up to 100-fold enhancements of fluorescence because TO becomes fluorescent as stacking interactions prevent twisting of the π-systems and because the rigidity of the formed duplex hampers quenching by donor–acceptor contact.

We deliberately sought a method that would allow the detection of pM quantities of DNA or RNA targets. Such a method may allow the direct detection of less abundant nucleic acid targets, for example in cells and cell lysates. Our preliminary work provided proof of the concept, yet the NIR664 dye used in the previous study interacted with the TO (donor) fluorophore in both the single stranded state (*via* contact quenching) and in the double stranded state (*via* FRET).[46] The disadvantage is that donor emission of TO/NIR664-labelled probes is significantly darker than donor emission of TO-only probes. Similar effects have been observed for molecular beacons.[12] This will affect measurements in matrices that have a high fluorescence background. Furthermore, the emission spectrum of the TO-donor only partially overlaps with the absorbance spectrum of the NIR664-acceptor, which limits the brightness of the FRET-signal measured in the double stranded state. As a solution to this problem, we considered a dissection of the energy transfer pathways and sought dye combinations that either maximize (1) the TO fluorescence signaling or (2) the FRET signaling (see Fig. 1). The study revealed probes that are amongst the most sensitive hybridization probes reported. Detectable fluorescence signals were observed in real time at 40 pM concentration of the target.

Results and discussion

Design

We assumed that strong enhancement of TO emission should be obtainable when the acceptor dye permits or even enforces

collisional quenching in the single stranded form while prohibiting Förster energy transfer in the double stranded state. This called for hydrophobic acceptor dyes that show negligible overlap of their absorbance spectrum with the donor emission (Fig. 1b, quenched stemless beacons III). In contrast, a good spectral overlap should yield probes (Fig. 1b, FRET stemless beacons IV) that exhibit strong FRET signals in the double stranded state. This probe design is different from the typical approaches used in the design of "regular" dual label-based detection probes. The TO chromophore acts as a smart fluorescence donor that emits only when double-strand formation has occurred.

We investigated 18-mer PNA model sequences **A4**, **A7**, **A10** and **A13**, in which the donor and the acceptor dyes (A) were separated by 4, 7, 10 and 13 nucleotides, respectively (see Fig. 2). For maximization of TO (donor) fluorescence in quenched stemless beacons we tested ITCC, DY752, and NIR797 as acceptor dyes. The Alexa594, DY590, and ICC dyes were envisioned to enable efficient FRET in the double stranded state. For reason of comparison, we analyzed single TO labeled probes **4**, **7**, **10** and **13** (A = H in Fig. 2) as well as the previously reported NIR667 labeled stemless beacons. Each probe shared a common core sequence (see Fig. 2, underlined region) around the TO chromophore to ensure comparable donor fluorescence properties and approximately equal duplex stabilities. The solid-phase synthesis of single TO labeled probes (FIT-probes) has been previously described.[47] Probes **A4–A13** were prepared in analogy to the synthesis of TO-NIR664-labeled stemless beacons.[46] Briefly, the PNA conjugates were synthesized by using Fmoc/Bhoc-protected PNA-monomers. After coupling of the terminal Boc-Lys(Fmoc) building block the Fmoc protecting group was removed from the side chain and the second fluorophore was introduced. Finally the Bhoc and Boc protecting groups were removed upon the final TFA treatment which simultaneously released the probes from the solid support.

PNA

4 H-Lys-cgta-Aeg(TO)-atagccgatgccg-Gly-NH_2
A4 H-Lys(**A**)-cgta-Aeg(TO)-atagccgatgccg-Gly-NH_2
7 H-Lys-gtccgta-Aeg(TO)-atagccgtcg-Gly-NH_2
A7 H-Lys(**A**)-gtccgta-Aeg(TO)-atagccgtcg-Gly-NH_2
10 H-Lys-gtcagccgta-Aeg(TO)-atagccg-Gly-NH_2
A10 H-Lys(**A**)-gtcagccgta-Aeg(TO)-atagccg-Gly-NH_2
13 H-Lys-ccggtcagccgta-Aeg(TO)-atag-Gly-NH_2
A13 H-Lys(**A**)-ccggtcagccgta-Aeg(TO)-atag-Gly-NH_2

DNA

C4 5'-CGGCATCGGCTATTTACG-3'
C7 5'-CGACGGCTATTTACGGAC-3'
C10 5'-CGGCTATTTACGGCTGAC-3'
C13 5'-CTATTTACGGCTGACCGG-3'

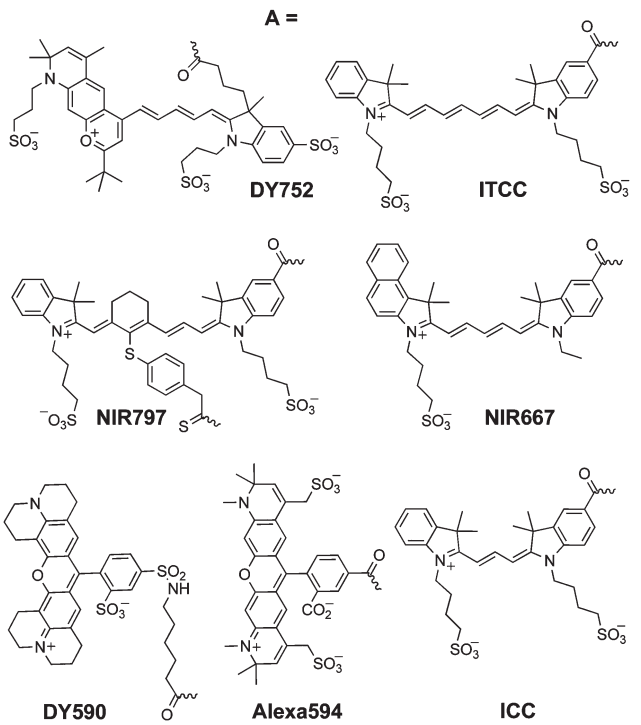

Fig. 2 Test sequences and acceptor dyes used in this study. Underlined regions are identical.

Hybridization experiments

A series of hybridization experiments was performed with the aim to identify donor–acceptor pairs and donor–acceptor distances that provide the highest intensification of fluorescence upon target binding. UV-monitored melt experiments revealed that the formed probe–target complexes had high stability (T_m > 75 °C), at least for the acceptor dyes tested (Fig. S36†). The fluorescence spectra of the dual labeled and the single labeled FIT-probes were measured before and after hybridization with complementary targets (Fig. 3, Table 1, see also Fig. S37†). The investigation of the entire set of dual labeled probes revealed that each of the examined acceptor fluorophores efficiently quenched the already low TO fluorescence F_0 in the single stranded state. For example, in **ITCC-10**, the TO fluorescence intensity was reduced by about 99.6% when compared with TO-only probe **10** (Table 1, compare entries 3 and 27). The differences in the UV spectra of single stranded **ITCC-10** and target-bound **ITCC-10·C10** suggested that the efficient quenching of TO-emission is the result of ground state TO–ITCC interactions (Fig. S38b†). Intramolecular dye–dye interactions have been observed previously in DNA-based probes.[48]

Hybridization with the complementary target was accompanied by dramatic increases of TO emission. It became apparent that the introduction of the second chromophore in PNA FIT-probes conferred remarkable improvements to fluorescence signaling F/F_0. For example, the single TO-labeled probe **13** experienced F/F_0 = 10-fold enhancements of TO emission upon addition of a target (Fig. 3a, entry 4 in Table 1). The introduction of an ITCC chromophore in **ITCC-13** led to a noteworthy fluorescence enhancement F/F_0 = 236 upon target binding (Fig. 3b, entry 28 in Table 1). The highest increase in TO fluorescence upon hybridization F/F_0 was determined when both dyes were separated by 10 nucleotides. This behavior was

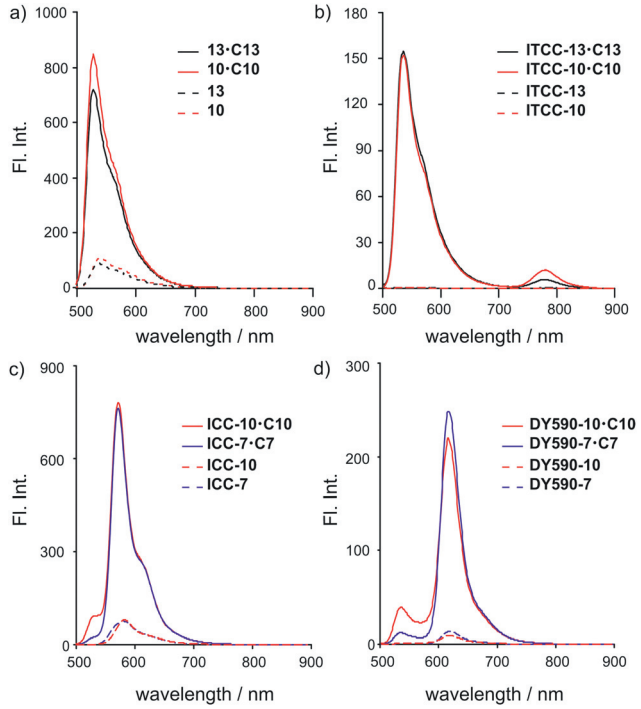

Fig. 3 Fluorescence spectra of probes before (dashed line) and after hybridization (solid line) with the target. Measurement conditions: see Table 1.

observed for all dye combinations. Very high signal-to-background ratios of approximately 10^2 were reached for ITCC, NIR664 and for the Alexa594 dye (F/F_0 = 450, 235 and 120, respectively). Of note, the hybridization-induced intensification of TO fluorescence F/F_0 was 10–40 times higher for TO/ITCC, TO/NIR664 and TO/Alexa594 combinations than for the corresponding single labeled probe **10**.

We next explored the FRET-based signaling of hybridization. In the single stranded state, significant FRET signals were measured for acceptor dyes (ICC, DY590, Alexa594) that provided efficient overlap between donor emission and acceptor absorbance while little background fluorescence was seen for dyes (NIR664, DY752, ITCC, NIR797) that absorbed far away from the TO emission. Most probes showed strong increases of the FRET signal upon hybridization. There was no clear trend of FRET signaling as far as the dependence on the distance between donor and acceptor is concerned. However, a 7 or 10 nucleotide distance seemed to provide a high responsiveness on average.

This probably reflects the need for an optimal co-alignment in the double helical probe–target complex. Dyes that were selected for FRET-maximization showed high intensities of acceptor emission. Please note, the TO/ICC-probes **ICC-4–ICC-13** provided exceptionally high intensities of acceptor signals: as bright as the donor emission in TO-only probes **4–13**. The DY590, Alexa594 and NIR664 acceptors showed a very high responsiveness (F/F_0 up to 250) combined with high intensities of FRET signals. High FRET fluorescence increases were also obtained for ITCC as the acceptor, but the absolute fluorescence intensities were very low.

This study exposed two particularly interesting dye combinations. The TO–ITCC pair conferred very high increases of TO emission F/F_0 (up to 450-fold) while the TO–ICC pair furnished surprisingly bright acceptor signals. The ITCC dye is a remarkably efficient quencher of the TO emission. The UV spectra are indicative of TO–ITCC ground state interactions (Fig. S38b†). In the single stranded state, more than 99% of TO emission was quenched regardless of the dye–dye distance (Table 2). Thus, the single strands **ITCC-4–ITCC-13** are exceptionally dark as evidenced by the low quantum yields (0.0004–0.0009) of TO emission. The addition of the complementary target led to dramatic enhancements of the brightness probably because rigidity prevents contacts between the two dyes. However, the broad TO emission profile facilitated energy transfer even within the duplex form. Although quenching of TO emission became less efficient when the dye–dye distance was increased, the presence of ITCC reduced the brightness of TO emission. This may complicate measurements in biological fluids with a high fluorescence background but will not affect applications involving the use of prepurified samples such as PCR samples or cell extracts (*vide infra*). Bright emission was obtained when the TO/ICC-probes **ICC-4–ICC-13** were used. The high efficiency of quenching of TO emission in both the single stranded (99%) and the target-bound form (89–97%) as well as the remarkable brightness (up to 35 000 L mol^{-1} cm^{-1}) of acceptor emission upon donor excitation suggest efficient energy transfer. The partial overlap of TO and ICC absorption spectra (Fig. S38a†) results in a remarkably high extinction coefficient ε_{485}. Thus direct excitation of the ICC dye on the one hand reduces the responsiveness of the probe but on the other hand contributes to the brightness of emission, which can be higher than emission of TO only probes (*vide infra*, Fig. 6).

Temperature dependence

Nucleic acid detection is performed in many different formats and at different hybridization temperatures. For example, the temperature ranges applied in the detection of target DNA during real-time PCR analysis significantly differ from the temperature requirements of measurements in live cells. It is, for this reason, important to examine the temperature dependence of the fluorescence responses. The measurements revealed a remarkably broad temperature range in which the TO/NIR664 pair provided high enhancements of TO fluorescence F/F_0 (Fig. 4a). By contrast, the TO/ICC combination showed a marked temperature dependence due to the increase of single strand emission at $T \geq$ 55 °C (Fig. S39c†). Of note, the high ($\geq 10^2$-fold) fluorescence increases F/F_0 conferred by the ITCC, NIR664 and Alexa594 acceptors remained high (≥200-fold) at $T \approx$ 60 °C. We conclude that these dual labeled PNA FIT-probes would allow measurement at room temperature, physiological temperature or at the elevated temperature typically used in real-time PCR measurements (annealing at 60 °C).

The FRET signals showed a markedly different temperature dependence (Fig. 4b). A pronounced maximum became apparent for most dyes. The ratio F/F_0 between FRET signals furnished in the presence and absence of a target was highest at $T \approx$ 35 °C, a temperature which is frequently applied in studies of living

Table 1 Fluorescence properties of single-stranded probes and probes after hybridization measured after excitation of the donor fluorescence (λ_{ex} = 485 nm). Measurement conditions: 1 μM probe, 1 μM target in 10 mM NaH_2PO_4, 100 mM NaCl at pH = 7.0, 25 °C

		Fluorescence[a] (λ_{em} = 530 nm)				Fluorescence[a,c] (FRET)		
Entry	Probe	F_0	F	F/F_0[b]	λ_{em} (FRET)	F_0	F	F/F_0[b] (FRET)
1	**4**	113.5	746.14	7				
2	**7**	84.0	896.5	11				
3	**10**	86.7	874.1	11				
4	**13**	73.5	750.9	10				
5	**ICC-4**	1.4	22.3	16	567 nm	65.4	805	12
6	**ICC-7**	1.2	23.9	19	567 nm	62.1	712	12
7	**ICC-10**	0.9	92.0	97	567 nm	46.2	737	16
8	**ICC-13**	1.0	56.1	56	567 nm	40.5	426	11
9	**DY590-4**	0.4	1.5	4	618 nm	17.3	18.4	1
10	**DY590-7**	0.7	11.0	16	618 nm	13.5	248	18
11	**DY590-10**	0.9	35.3	41	618 nm	9.1	218	24
12	**DY590-13**	1.3	53	41	618 nm	16.7	65.8	4
13	**Alexa594-4**	3.4	256.2	75	630 nm	21.2	67.2	3
14	**Alexa594-7**	1.3	134.9	102	630 nm	22.8	389	17
15	**Alexa594-10**	0.8	98.8	120	630 nm	64.1	227	4
16	**Alexa594-13**	4.5	88.3	28	630 nm	96.0	97.4	1
17	**NIR664-4**	4.4	51.9	12	695 nm	4.0	152	38
18	**NIR664-7**	6.9	90.5	13	695 nm	2.7	115	43
19	**NIR664-10**	0.4	94.1	235	695 nm	0.2	50.8	254
20	**NIR664-13**	0.7	155.9	223	695 nm	3.1	40.4	13
21	**DY752-4**	15.8	95.8	6	760 nm	0.2	0.3	2
22	**DY752-7**	3.0	34.5	12	760 nm	4.0	18.6	5
23	**DY752-10**	2.3	117.1	51	760 nm	3.3	23.7	7
24	**DY-75213**	8.6	126.1	15	760 nm	2.0	1.7	1
25	**ITCC-4**	0.5	26.3	53	780 nm	0.3	13.8	46
26	**ITCC-7**	0.6	51.3	86	780 nm	0.1	18.3	183
27	**ITCC-10**	0.3	135.7	452	780 nm	0.1	11.9	119
28	**ITCC-13**	0.6	141.6	236	780 nm	0.3	5.7	19
29	**NIR797-4**	3.7	15.7	4	817 nm	0.1	0.3	3
30	**NIR797-7**	1.8	64.0	35	817 nm	0.1	0.3	3
31	**NIR797-10**	2.7	179.0	66	817 nm	0.1	0.3	3
32	**NIR797-13**	1.7	58.5	35	817 nm	0.1	0.3	2

[a] F_0, fluorescence intensity of single stranded probes; F, fluorescence intensity of probes after addition of complementary DNA. [b] Standard deviation: 16% of mean for F/F_0 = 1–10; 5–10% for F/F_0 = 10–100. [c] Measured for acceptor emission.

Table 2 Photophysical properties of ICC and ITCC labelled PNA FIT-probes before and after hybridization. Measurement conditions: see Table 1

	QE[a]	ϕ_{em}[b]	ε_{485}[c]/L mol^{-1} cm^{-1}
ITCC-4	0.996	0.001	53 000
ITCC-4·C4	0.965	0.023	46 000
ITCC-7	0.993	0.001	60 000
ITCC-7·C7	0.943	0.046	57 000
ITCC-10	0.997	0.001	60 000
ITCC-10·C10	0.845	0.132	49 000
ITCC-13	0.992	0.001	50 000
ITCC-13·C13	0.811	0.108	63 000
ICC-4	0.988	0.036	107000
ICC-4·C4	0.970	0.357	91000
ICC-7	0.986	0.028	103000
ICC-7·C7	0.973	0.322	109000
ICC-10	0.990	0.035	104000
ICC-10·C10	0.895	0.287	111000
ICC-13	0.896	0.028	94000
ICC-13·C13	0.925	0.308	99000

[a] Quenching efficiency QE = 1 − F_{530} (donor/acceptor labeled)/F_{530} (donor labeled), error estimated as 10%. [b] Quantum yield measured at emission maximum (TO emission for ITCC probes, ICC emission for ICC probes), error estimated as 10%. [c] Error estimated as 10%, please note, the TO extinction coefficient is dependent on the next neighbours.[24]

systems. The responsiveness rapidly dropped at elevated temperatures. Among the FRET pairs studied, the TO/Alexa594 and the TO/ICC combination displayed the highest tolerance to high temperatures as more than 50% of the maximum responsiveness was maintained between 20 and 50 °C. Thus, the ICC acceptor not only provided exceptionally bright FRET signals but also offered a reasonable temperature tolerance in a range that enables measurements in cells.

Sensitivity of DNA detection

The gain of signal F/F_0 obtained upon target binding is a key parameter that determines the sensitivity of the assay required that (a) the affinity of the probe for the target is sufficiently high to enable complex formation at low target concentrations and (b) the measured fluorescence intensity significantly exceeds noise. The stemless beacons described in Table 1 provide high T_m values ($T_m \approx 80$ °C, see Fig. S36†), low intensity of TO emission in the absence of a target (=low background) and >10^2-fold enhancements of TO fluorescence upon hybridization with the target. The TO–ITCC pair conferred particularly high increases of TO emission F/F_0 (up to 450-fold). This suggested that dual

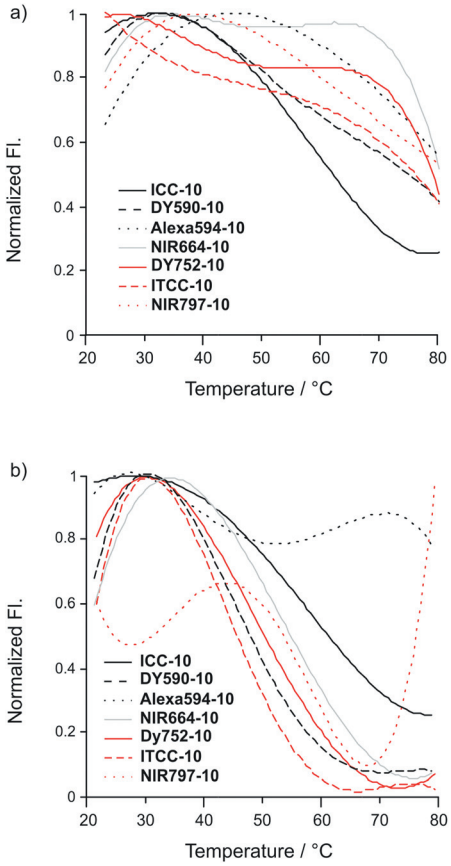

Fig. 4 Temperature dependence of fluorescence enhancement upon hybridization illustrated as normalized fluorescence enhancement $(F/F_0)/(F/F_0)_{max}$ for (a) the TO fluorescence signaling and (b) the FRET signaling. Emission in (a) was measured at maximum of donor fluorescence (TO signal) and in (b) at the maximum of the acceptor dye fluorescence (FRET signal). Measurement conditions, see Table 1, heating rate 1 °C min^{-1}.

label PNA FIT-probes such as **ITCC-10** should furnish measurable increases of fluorescence at low target:probe ratios. The TO/ITCC-containing probe **ITCC-10** was titrated with increasing amounts of target. The fluorescence was measured by using conventional cuvettes and a conventional fluorescence spectrometer. A 100 nM probe concentration significantly exceeds the K_d of the probe–target complex and therefore provides the desired linear characteristics of an active site titration (Fig. 5a). The gain of fluorescence $F - F_0$ surpassed the threefold of the error of the mean when 40 pM target was added (Fig. 5b). Thus, probes such as **ITCC-10** can detect <0.001 eq target. For comparison, recent investigations in fluorescent hybridization probes have described calculated detection limits in the range of 1 nM target for "conventional" molecular beacons,[15] 0.3 nM target with 100 nM excimer-controlled beacon,[19] 0.5 nM target for a mercury enhanced beacon[15] or a measured detection limit of 0.5 nM with 500 nM FIT-PNA.[30] Higher sensitivities have been obtained when probe–target recognition is used to trigger catalytic processes.[49–51] These methods register the formation of signaling molecules that accumulate over time, whereas methods that rely on a single hybridization probe such as **ITCC-10** provide signals without delay time.

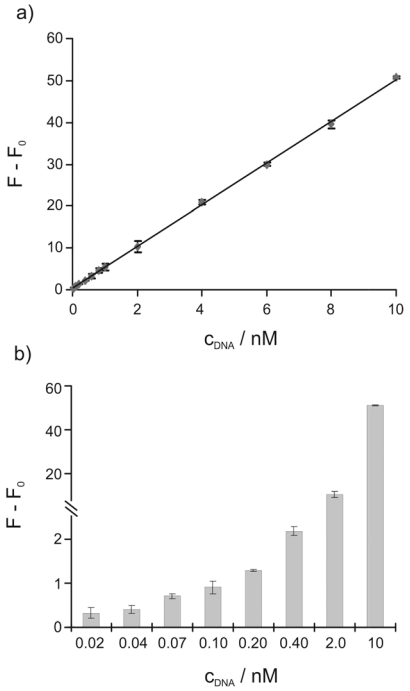

Fig. 5 Concentration dependence of fluorescence signal of probe·target-duplex **ITCC-10·C10**. Measurement conditions: 100 nM probe in 10 mM NaH_2PO_4, 100 mM NaCl buffer at pH = 7.0, 25 °C, λ_{ex} = 485 nm, λ_{em} = 530 nm.

RNA detection

In a recent study, we showed that the single TO-labelled probe **NA10** allowed the detection and localization of intracellular viral mRNA coding for neuraminidase of influenza A (H1N1).[31] We used this probe sequence to further examine the signaling improvements conferred by dual labeling. Based on the high values of the signal-to-background F/F_0 and the extraordinary brightness of FRET emission, we decided to equip the stemless PNA beacon with the TO/ITCC pair in **ITCC-NA10** and the TO/ICC pair in **ICC-NA10**, respectively. The probe sequence was designed in analogy to the sequence of molecular beacon **MB_NA** which has previously been used for the detection of influenza RNA in live cells.[52] The acceptor dyes ITCC or ICC were attached to the C-terminal lysine side chain at 10 nt distance to the TO donor. Under the conditions chosen, the single labeled probe **NA10** furnished an 8-fold increase of fluorescence (Fig. 6a). The ITCC-label in **ITCC-NA10** improved, again, the responsiveness of TO fluorescence. TO-emission of the probe–target complex was 40-fold brighter than the TO-emission of the single-stranded probe **ITCC-NA10** (Fig. 6c). In comparison, the TAMRA/DABCYL-labeled molecular beacon **MB_NA** provided 11-fold enhancements of donor fluorescence upon RNA hybridization (Fig. 6b). The hybridization of the TO/ICC-labeled stemless beacon **ICC-NA10** showed, again, bright emission signals, which is due to FRET and direct excitation of ICC at the selected excitation wavelength (Fig. 6d).

In this study, it was the aim to develop molecular beacon-type hybridization probes that enable the homogeneous detection of DNA and RNA targets that occur at low abundance. A sensitive molecular beacon is characterized by a low fluorescence

5'-TAMRA-GCGACTTTCAGTTATTATGCCGTTGTATTTGTCGC-DABCYL-3', **MB-NA**
5'-AAAUACAACGGCAUAAUAACUGAAA-3', **RNA1**
H-Lys-cagtta-Aeg(TO)-tatgccgttg-A,
A = H, **NA10**; A = Lys(ITCC)-NH_2, **ITCC-NA10**; A = Lys(ICC)-NH_2, **ICC-NA10**
5'-CAACGGCAUAAUAACUG-3', **RNA2**

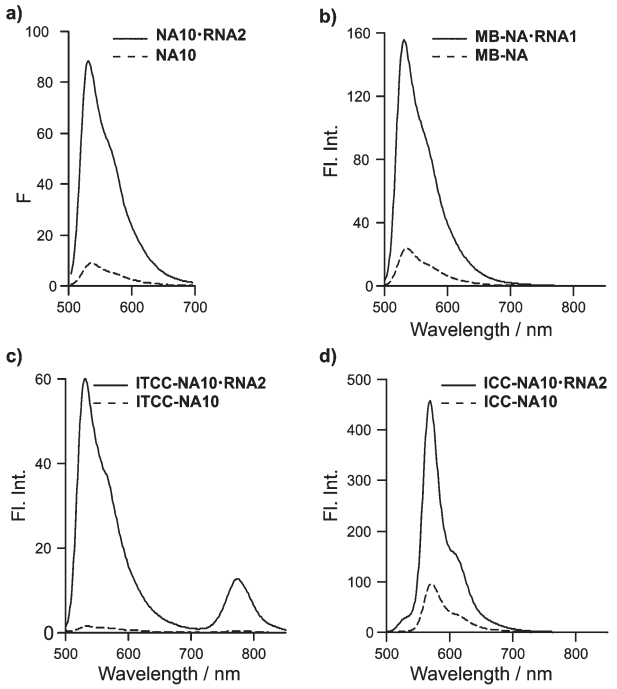

Fig. 6 Fluorescence spectra of (a) **NA10**, (b) **MB_NA,** (c) **ITCC-NA10**, and (d) **ICC-NA10** before (dashed lines) and after addition (solid lines) of (a) matched **RNA1** or (b), (c), and (d) matched **RNA2**. Measurement conditions: 1 μM probe, 1 μM target when added in 10 mM NaH_2PO_4, 100 mM NaCl at pH = 7.0, 25 °C, λ_{ex} = 485 nm.

background F_0. Thus, the beacon design must enforce dye–dye interactions in the single stranded state. The dual-labeled PNA probes presented in here enabled up to 99.8% quenching of the TO emission measured in the double stranded state. This is accomplished despite the absence of a stem sequence. Similar quenching efficiencies (99.7%) have been achieved with super-quenched DNA molecular beacons, which require multiple labels and a stem segment to enhance the donor–acceptor contact.[12] The PNA scaffold not only facilitates intramolecular dye–dye interactions (in the single stranded state), it also confers high affinity ($T_m \geq 80$ °C of 18-mer probes). High affinities help the quantitative formation of probe–target complexes which otherwise can be difficult to assure when very low target concentrations are to be detected. However, this will be of little use if the presence of the quencher reduces brightness of fluorescence F in the target-bound form. The near-infrared-labeled PNA FIT-probes such as **ITCC-10** or **NIR797-10** minimize quenching in the double-stranded state because collisions between the TO donor and the acceptors are hindered by means of donor intercalation and the rigidity of the probe–target duplex. A regular molecular beacon has a dissociated stem region when bound to the target. Thus, the dye labeled termini gain degrees of freedom upon target binding. As a result, the average dye–dye distance in target-bound molecular beacons may be shorter than the dimension of the probe–target duplex. This can lead to low intensities of donor emission. Shared-stem molecular beacons,[53] in-stem molecular beacons[16–18] and the FRET based stemless beacons such as **ICC-10** present solutions to this problem. The dual labeled PNA FIT-probes such as **ITCC-10** afforded detectable signals at 10^{-11} M target concentration, which compares favorably with the detection limits described for alternative molecular beacons. The reduced fluorescence background and the increased brightness of TO/ICC-labeled probes is a significant improvement of our previous FIT-probes.[46]

The collected data suggest that dual label PNA FIT-probes which contain thiazole orange as an artificial nucleobase provide a suitable platform for the design of FRET systems. One reason is that probe–target recognition is required to activate the latent donor abilities of TO. Second, the sequence-internal incorporation of the fluorescence donor probably facilitates the adjustment of the donor–acceptor distance. We have shown that 4–10 nt distance provides highest enhancements of FRET emission upon hybridization. The nucleotide spacer that separates donor and acceptor dyes in the dual label PNA FIT-probes is shorter than in regular molecular beacons. Despite this comparably small donor–acceptor distance, the intercalated TO donor is protected from collisions with the acceptor dye.

Conclusions

We have developed dual-labeled PNA-based beacons that facilitate the detection of low copy number DNA/RNA targets. The probes provided up to 450-fold enhancements of fluorescence intensity upon target binding. In contrast to existing DNA-based molecular beacons, this PNA beacon platform does not require a stem sequence to enforce dye–dye communication. Rather, the method relies on the energy transfer between a "smart" thiazole orange (TO) dye, which requires formation of the probe–target complex in order to become fluorescent, and a terminally appended acceptor dye. Moreover, the mechanism of energy transfer changes, upon hybridization, from collisional quenching in the single-stranded state to Förster-type transfer in the double-stranded state. The PNA beacon platform allows various read-out methods. We dissected the energy transfer pathways and explored dye combinations that either maximize (1) the TO fluorescence signaling or (2) the FRET signaling. The study revealed that hydrophobic and polarizable acceptor dyes that show little overlap between TO emission spectra and acceptor absorption spectra improved the responsiveness of donor emission. The use of near-infrared dyes such as NIR664 and the heptamethine cyanine ITCC led to donor–acceptor ground state interactions which diminished background fluorescence F_0 by 99.97% (of the maximum intensity of donor emission of a sequence-identical donor-only labeled probe). Hybridization of the essentially dark probes disrupts the dye–dye interaction and the emission of the TO donor dramatically increases by up to 450-fold provided that the donor and the acceptor are separated by 10–13 nucleotides. The high fractional increase of fluorescence upon target addition enabled the very sensitive detection of DNA targets (40 pM LOD), which was detectable at less than 0.1% of the beacon concentration. Dual label PNA FIT-probes are a suitable platform to achieve responsive and bright FRET emission. Despite spectral overlap of TO donor emission with acceptor

excitation, fluorescence of single stranded probes is low because torsional motions around the methane bridge in TO lead to depletion of the TO donor excited state and because the flexibility of PNA facilitates quenching *via* dye–dye contacts. These quenching modes are hindered in the target-bound state. Thus, the formation of the probe–target complex is accompanied by enhancements of the FRET signal. Acceptor emission was measured at various wavelengths (ICC at 567 nm, DY590 at 618 nm, Alexa594 at 630 nm, NIR664 at 695 nm) which suggests applications in multiplex assays. The trimethine cyanine ICC provided particularly high intensities of emission *via* FRET provided that the donor–acceptor distance does not exceed 10 nucleotides. The brightness of the FRET signal and the large apparent Stokes shift (82 nm) suggests applications in the detection of specific RNA targets in biogenic matrices without the need of sample pre-processing prior to detection.

Experimental section

Materials

Fmoc protected PNA monomers were purchased from ASM Chemical Research. DNA (salt free) was purchased from BioTeZ Berlin-Buch GmbH, Germany. RNA was purchased from Life Technologies Ltd (Paisley, UK). The dyes DY590 and DY752 were purchased from Dyomics (Jena, Germany), the dye Alexa-Fluor 594 was purchased from Life Technologies GmbH (Darmstadt, Germany), the dyes ICC and ITCC were purchased from Mivenion (Berlin, Germany), and the dyes NIR664 and NIR797 were purchased from Fluka (Merck Biosciences, Germany). Water was purified with an Astacus Water Purification System (Membrapure GmbH, Germany).

Solid phase synthesis, purification and characterization

Automated linear solid phase synthesis was performed by using an Intavis ResPep parallel synthesizer equipped with micro scale columns for PNA synthesis. The NovaSyn®-TRG resin was purchased from Novabiochem (Merck Biosciences, Germany). For details of probe synthesis, see the ESI.† HPLC was performed with an Agilent 1100 series instrument using a Varian Polaris-C18 A 5µ (PN A 2000-250x046) at 55 °C or a Varian Polaris-C18 A 5µ (PN A 2000-1254/2) at 55 °C for analytical runs and a Varian Polaris C18 A 5µ (PN A 2000-250-100) for semi-preparative runs. Eluents analytical: A (0.1% HCOOH in water + 1% MeCN) and B (0.1% HCOOH in MeCN + 1% water); semi-preparative: A (0.1% TFA in water + 1% MeCN) and B (0.1% TFA in MeCN + 1% water) were used in a linear gradient with a flow rate of 1 mL min^{-1} for analytical and 6 mL min^{-1} for semi-preparative HPLC. For probe characterization, the optical density was measured at 260 nm with a Varian Cary Bio-UV/Vis spectrometer by using 100 µl quartz cuvettes 105.200-QS from Hellma. The extinction coefficients were calculated by applying the nearest neighbor method and oligo calculation was carried out by using the script from Proligo (http://proligo2.proligo.com). Measurements of absorption at 260 nm were carried out in a buffer solution (100 mM NaCl, 10 mM NaH_2PO_4, pH 7) at ambient temperature. The sample concentration was calculated by approximating for thiazole orange ε_{260}(TO) ≈ ε_{260}(thymine) and for other chromophores ε_{260}(NIR667) ≈ ε_{260}(adenine). Stock solutions of stemless beacons and short synthetic DNA have a concentration of 1 mM and were stored at −20 °C. MALDI-TOF mass spectra were recorded by using a Voyager-DE Pro Biospectrometry Workstation of PerSeptive Biosystems.

Fluorescence measurements

Fluorescence spectra were recorded by using a Varian Cary Eclipse spectrometer. Measurements of single labeled probes were carried out in 1 mL semi-micro fluorescence quartz cuvettes 108F-QS from Hellma. Measurements of dual labeled PNA probes were carried out in 100 µL ultra-micro fluorescence cuvettes 105.250-QS from Hellma and the solution was covered with 200 µL of mineral oil. If not mentioned otherwise fluorescence emission was detected in a 1 µM concentration buffered solution (100 mM NaCl, 10 mM NaH_2PO_4, pH 7) and excitation at 485 nm for TO; $Slit_{Ex}$ = 10 nm, $Slit_{Em}$ = 5 nm. After addition of DNA or RNA to the probe, solutions were heated to 95 °C for 1 min before cooling to 25 or 60 °C. Spectra were recorded after 5 min at 25 °C. Buffer-only fluorescence was subtracted.

Notes and references

1 D. M. Kolpashchikov, *Chem. Rev.*, 2010, **110**, 4709–4723.
2 R. T. Ranasinghe and T. Brown, *Chem. Commun.*, 2005, 5487–5502.
3 S. Tyagi and F. R. Kramer, *Nat. Biotechnol.*, 1996, **14**, 303–308.
4 K. M. Wang, Z. W. Tang, C. Y. J. Yang, Y. M. Kim, X. H. Fang, W. Li, Y. R. Wu, C. D. Medley, Z. H. Cao, J. Li, P. Colon, H. Lin and W. H. Tan, *Angew. Chem., Int. Ed.*, 2009, **48**, 856–870.
5 X. H. Fang, X. J. Liu, S. Schuster and W. H. Tan, *J. Am. Chem. Soc.*, 1999, **121**, 2921–2922.
6 J. A. M. Vet, A. R. Majithia, S. A. E. Marras, S. Tyagi, S. Dube, B. J. Poiesz and F. R. Kramer, *Proc. Natl. Acad. Sci. U. S. A.*, 1999, **96**, 6394–6399.
7 L. G. Kostrikis, S. Tyagi, M. M. Mhlanga, D. D. Ho and F. R. Kramer, *Science*, 1998, **279**, 1228–1229.
8 G. Leone, H. van Schijndel, B. van Gemen, F. R. Kramer and C. D. Schoen, *Nucleic Acids Res.*, 1998, **26**, 2150–2155.
9 D. L. Sokol, X. L. Zhang, P. Z. Lu and A. M. Gewitz, *Proc. Natl. Acad. Sci. U. S. A.*, 1998, **95**, 11538–11543.
10 S. Tyagi, S. A. E. Marras and F. R. Kramer, *Nat. Biotechnol.*, 2000, **18**, 1191–1196.
11 P. Zhang, T. Beck and W. H. Tan, *Angew. Chem., Int. Ed.*, 2001, **40**, 402–405.
12 C. Y. J. Yang, H. Lin and W. H. Tan, *J. Am. Chem. Soc.*, 2005, **127**, 12772–12773.
13 B. Dubertret, M. Calame and A. J. Libchaber, *Nat. Biotechnol.*, 2001, **19**, 365–370.
14 T. N. Grossmann, L. Röglin and O. Seitz, *Angew. Chem., Int. Ed.*, 2007, **46**, 5223–5225.
15 Y. W. Lin, H. T. Ho, C. C. Huang and H. T. Chang, *Nucleic Acids Res.*, 2008, 36.
16 Y. Hara, T. Fujii, H. Kashida, K. Sekiguchi, X. G. Liang, K. Niwa, T. Takase, Y. Yoshida and H. Asanuma, *Angew. Chem., Int. Ed.*, 2010, **49**, 5502–5506.
17 H. Kashida, T. Takatsu, T. Fujii, K. Sekiguchi, X. G. Liang, K. Niwa, T. Takase, Y. Yoshida and H. Asanuma, *Angew. Chem., Int. Ed.*, 2009, **48**, 7044–7047.
18 C. Holzhauser and H. A. Wagenknecht, *Angew. Chem., Int. Ed.*, 2011, **50**, 7268–7272.
19 R. Häner, S. M. Biner, S. M. Langenegger, T. Meng and V. L. Malinovskii, *Angew. Chem., Int. Ed.*, 2010, **49**, 1227–1230.
20 S. Berndl and H. A. Wagenknecht, *Angew. Chem., Int. Ed.*, 2009, **48**, 2418–2421.
21 S. M. Biner, D. Kummer, V. L. Malinovskii and R. Haner, *Org. Biomol. Chem.*, 2011, **9**, 2628–2633.

22 P. Conlon, C. Y. J. Yang, Y. R. Wu, Y. Chen, K. Martinez, Y. M. Kim, N. Stevens, A. A. Marti, S. Jockusch, N. J. Turro and W. H. Tan, *J. Am. Chem. Soc.*, 2008, **130**, 336–342.
23 L. Bethge, D. V. Jarikote and O. Seitz, *Bioorg. Med. Chem.*, 2008, **16**, 114–125.
24 D. V. Jarikote, N. Krebs, S. Tannert, B. Röder and O. Seitz, *Chem.–Eur. J.*, 2007, **13**, 300–310.
25 O. Köhler, D. V. Jarikote and O. Seitz, *ChemBioChem*, 2005, **6**, 69–77.
26 O. Köhler and O. Seitz, *Chem. Commun.*, 2003, 2938–2939.
27 O. Seitz, F. Bergmann and D. Heindl, *Angew. Chem., Int. Ed.*, 1999, **38**, 2203–2206.
28 V. Karunakaran, J. L. F. Lustres, L. J. Zhao, N. P. Ernsting and O. Seitz, *J. Am. Chem. Soc.*, 2006, **128**, 2954–2962.
29 A. Tonelli, T. Tedeschi, A. Germini, S. Sforza, R. Corradini, M. C. Medici, C. Chezzi and R. Marchelli, *Mol. BioSyst.*, 2011, **7**, 1684–1692.
30 E. Socher, D. V. Jarikote, A. Knoll, L. Röglin, J. Burmeister and O. Seitz, *Anal. Biochem.*, 2008, **375**, 318–330.
31 S. Kummer, A. Knoll, E. Socher, L. Bethge, A. Herrmann and O. Seitz, *Angew. Chem., Int. Ed.*, 2011, **50**, 1931–1934.
32 A. G. Torres, M. M. Fabani, E. Vigorito, D. Williams, N. Al-Obaidi, F. Wojciechowski, R. H. E. Hudson, O. Seitz and M. J. Gait, *Nucleic Acids Res.*, 2012, **40**, 2152–2167.
33 Y. Kam, A. Rubinstein, A. Nissan, D. Halle and E. Yavin, *Mol. Pharmaceutics*, 2012, **9**, 685–693.
34 N. Svanvik, J. Nygren, G. Westman and M. Kubista, *J. Am. Chem. Soc.*, 2001, **123**, 803–809.
35 N. Svanvik, G. Westman, D. Y. Wang and M. Kubista, *Anal. Biochem.*, 2000, **281**, 26–35.
36 S. Ikeda and A. Okamoto, *Chem.–Asian J.*, 2008, **3**, 958–968.
37 A. Okamoto, *Chem. Soc. Rev.*, 2011, **40**, 5815–5828.
38 F. Menacher, M. Rubner, S. Berndl and H. A. Wagenknecht, *J. Org. Chem.*, 2008, **73**, 4263–4266.
39 C. Holzhauser, S. Berndl, F. Menacher, M. Breunig, A. Gopferich and H. A. Wagenknecht, *Eur. J. Org. Chem.*, 2010, 1239–1248.
40 S. Berndl, M. Breunig, A. Gopferich and H. A. Wagenknecht, *Org. Biomol. Chem.*, 2010, **8**, 997–999.
41 L. Bethge, I. Singh and O. Seitz, *Org. Biomol. Chem.*, 2010, **8**, 2439–2448.
42 U. Asseline, M. Chassignol, Y. Aubert and V. Roig, *Org. Biomol. Chem.*, 2006, **4**, 1949–1957.
43 O. Seitz, *Angew. Chem., Int. Ed.*, 2000, **39**, 3249–3252.
44 H. Kuhn, V. V. Demidov, B. D. Gildea, M. J. Fiandaca, J. C. Coull and M. D. Frank-Kamenetskii, *Antisense Nucleic Acid Drug Dev.*, 2001, **11**, 265–270.
45 H. Kuhn, V. V. Demidov, J. M. Coull, M. J. Fiandaca, B. D. Gildea and M. D. Frank-Kamenetskii, *J. Am. Chem. Soc.*, 2002, **124**, 1097–1103.
46 E. Socher, L. Bethge, A. Knoll, N. Jungnick, A. Herrmann and O. Seitz, *Angew. Chem., Int. Ed.*, 2008, **47**, 9555–9559.
47 D. V. Jarikote, O. Köhler, E. Socher and O. Seitz, *Eur. J. Org. Chem.*, 2005, 3187–3195.
48 M. K. Johansson and R. M. Cook, *Chem.–Eur. J.*, 2003, **9**, 3466–3471.
49 L. Zhu and E. V. Anslyn, *Angew. Chem., Int. Ed.*, 2006, **45**, 1190–1196.
50 T. N. Grossmann, A. Strohbach and O. Seitz, *ChemBioChem*, 2008, **9**, 2185–2192.
51 P. Scrimin and L. J. Prins, *Chem. Soc. Rev.*, 2011, **40**, 4488–4505.
52 W. Wang, Z. Q. Cui, H. Han, Z. P. Zhang, H. P. Wei, Y. F. Zhou, Z. Chen and X. E. Zhang, *Nucleic Acids Res.*, 2008, **36**, 4913–4928.
53 A. Tsourkas, M. A. Behlke and G. Bao, *Nucleic Acids Res.*, 2002, **30**, 4208–4215.